ANALYSIS OF ELASTIC–PLASTIC BEHAVIOR OF A STEEL BRACE SUBJECTED TO REPEATED AXIAL FORCE

MICHIO SHIBATA

Department of Architecture, Osaka Institute of Technology Omiya 5-16-1, Asahi-ku, Osaka, Japan

Abstract—A practical method of analyzing a brace under repeated axial force is presented. A closed-form solution has been derived for a bar of ideal I-section with bi-linear stress–strain relationship, and the solution for the elastic-perfectly plastic bar shows good agreement with the exact solution by Nonaka For a bar of arbitrary solid cross-section with piecewise linear stress–strain relationship, an incremental load-displacement relationship has been obtained in an analytical form The computed results agrees reasonably well with the experimental results and with detailed finite element solution

1. INTRODUCTION

A brace, one of the most important earthquake-resistant elements of a steel structure, is subjected to alternately repeated axial forces by the earthquake. Because the initial rigidity and strength of the brace are much greater than those of the frame elements in a braced frame, it is essential to study the accurate axial force-displacement relationship of a single brace to investigate the elastic–plastic behavior of braced frames.

A number of theoretical investigations of the hysteretic behavior of a single brace have been made in the last decade, and can be classified into two categories. The first approach is to obtain analytical solutions using the plastic hinge concept in which the material yielding is concentrated in a critical section[1–7]; and the second is to use a numerical method based on the one- or two-dimensional continuum theory[8–12].

Although the plastic hinge analysis can yield closed-form solutions on some simple problems, because of the assumption of perfect plasticity, the influence of the Bauschinger's effect, the strain hardening, and the reversal of plastic strain should be ignored. The reduction of the sectional rigidity caused by the partial yielding is also ignored, which plays an important role on the post-buckling behavior

The numerical continuum analysis can be conducted by introducing the appropriate mathematical model and the precise constitutive relationship. However, except for some simple problems, it takes much time to compute the complicated interactions between braces and frame elements of a braced frame. The analysis requires solving simultaneous nonlinear equations so many times that it involves the risk that the iterative procedure does not converge.

In this study, we developed a practical method of analysis of the hysteretic behavior of a simply supported prismatic bar subjected to repeated axial force. The method holds reasonable accuracy with much less computing time than is required by the numerical continuum analysis. The bar is composed of two nonflexural straight segments and one elastic–plastic spring, whose mechanical property depends on the moment-curvature relation under varying axial force. The load-displacement relationship is obtained in a simple form, based on the detailed stress–strain relationship of the material.

2 ASSUMPTIONS

The general basic assumptions are: (1) the material is sufficiently dutile; (2) local instability does not occur; (3) although change in geometry is taken into account, deflection is so small that the square of the slope is negligibly small in comparison with unity.

The following idealizations are adopted: The simply supported bar of length $2L$ (Fig. 1a), is idealized into a model (Fig. 1b) composed of an elastic–plastic spring and two straight segments. The relative rotation 2θ of the spring is expressed by the curvature κ of the midsection, which
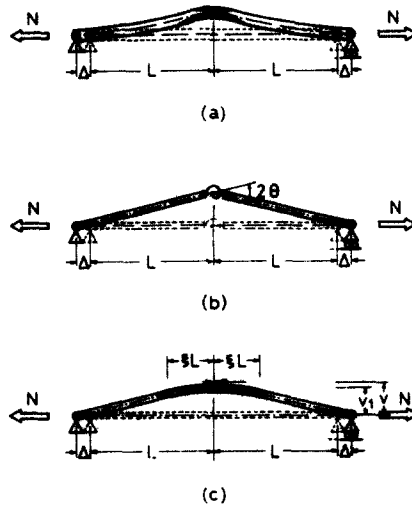
Fig 1. Analytical model

is determined by the axial force N and the bending moment $M = -Nv$ of the midsection, as follows:

$$\theta = \xi L \kappa \tag{1}$$

where ξ is a constant, independent of the loading history or the slenderness of the bar.

This idealization may be recognized as the generalized Shanley's model[13], and physically corresponds to the assumption that the curvature of the midsection is distributed uniformly over the length $2\xi L$ and that the remaining portions remain straight (Fig. 1c). ξ is estimated as $\xi = 1/3$ by which the total hysteretic behavior under repeated axial force is evaluated most accurately. This is discussed later.

A very short column does not buckle immediately when the axial compression attains the crush load; it plastically contracts to some extent without any lateral deflection. The axial force-displacement relation has a plastic plateau. Because the length of the plateau depends upon the distribution of cross-sectional imperfections and can not be determined definitely[14], it is also assumed that a compressed straight bar buckles when the compression reaches the Euler load, N_E or the current crush load. We exclude the case in which the bar-length is so short that the plastic plateau plays an important role in the total hysteretic behavior.

3 BASIC RELATIONSHIPS

Defining nondimensional parameters of axial force N and bending moment M of the midsection (Fig. 2), as $n \equiv N/N_0$, and $m \equiv M/M_0$, the equilibrium of the half bar, along with eqn (1), gives

$$m = -nk/n_c \tag{2}$$

where N_0 is the limit load in pure tension, M_0 is the limit moment in pure bending, $k \equiv EI/M_0\kappa$ is the nondimensional value of the curvature κ of the midsection, and $n_c \equiv EI/(\xi N_0 L^2)$ is the ratio of the elastic buckling load of the model to N_0 where E is Young's modulus and I is the moment of inertia of the cross section. The ratio of the Euler load to N_0, $n_E = \pi^2 EI/(4N_0 L^2)$, is related to n_c by $n_c = 4/(\xi \pi^2)n_E$ and, if $\xi = 4/\pi^2$, n_c agree with n_E.

Fig 2 Equilibrium of a half bar

Equation (2) can be written incrementally, without neglecting higher order terms, as

$$dm = -(n\,dk + k\,dn + dn\,dk)/n_c. \tag{3}$$

The definition of the stress resultants gives two incremental constitutive relationships at the midsection,

$$\begin{cases} dn = \bar{A}\,de + \alpha\bar{S}\,dk \\ dm = \bar{S}\,de + \bar{I}\,dk \end{cases} \tag{4}$$

where $de = d\varepsilon/\varepsilon_0$ denotes the ratio of the axial strain increment $d\varepsilon$ of the centroid to the initial yield strain ε_0, and $\alpha = Z_p^2/(AI)$ is a cross sectional parameter of sectional area A, plastic section modulus Z_p, and I. Values $\bar{A} = \int \mu\,dA/A$, $\bar{S} = \int y\mu\,dA/Z_p$ and $\bar{I} = \int y^2\mu\,dA/I$ are evaluated by integrating the ratio μ of the current tangent modulus of each fiber element to the Young's modulus, over the cross sectional area, where y denotes the distance between each fiber element and the centroid.

Eliminating dm from eqns (3) and (4), de and dn are written as simple functions of dk:

$$de = C_1\,dk + C_2(dk)^2/(1 + C\,dk)$$
$$dn = (C_1\bar{A} + \alpha\bar{S})\,dk + C_2\bar{A}(dk)^2/(1 + C\,dk) \tag{5}$$

where

$$C_1 = \frac{n_c\bar{I} + \alpha k\bar{S} + n}{k\bar{A} + n_c\bar{S}}, \quad C_2 = -\frac{C_1\bar{A} + \alpha\bar{S}}{k\bar{A} + n_c\bar{S}}, \quad C = \frac{\bar{A}}{k\bar{A} + n_c\bar{S}}$$

In the actual calculation, $\bar{A}$, $\bar{S}$ and $\bar{I}$ can be computed by dividing the midsection into a finite number of strip elements, assuming the uniform distribution of μ in a strip. If we also assume that the stress–strain relationship is piecewise linear, $\bar{A}$, $\bar{S}$ and $\bar{I}$ vary discretely with time and eqn (5) is valid for finite duration while $\bar{A}$, $\bar{S}$ and $\bar{I}$ remain constant, because the nonlinear term is not neglected in eqn (3).

To carry out accurate step-by-step computation, it is necessary to trace each branching point at which the stiffness distribution of the system changes. The nondimensional strain increment of the jth fiber element of midsection and that of the straight segment, taking into account eqn (4), are written as the functions of dk:

$$de_j = de + (Z_p/I)y_j\,dk = \{C_1 + (Z_p/I)y_j\}dk + C_2(dk)^2/(1 + C\,dk) \tag{6}$$

$$de_R = dn/\mu_R = \left\{(C_1\bar{A} + \alpha\bar{S})\,dk + \frac{C_2\bar{A}(dk)^2}{1 + C\,dk}\right\}\Big/\mu_R. \tag{7}$$

The necessary increment $d\tilde{e}$ of a certain fiber element, at which the fiber stiffness subsequently changes (Fig. 3), is determined from the constitutive relationship and the strain history. Substituting $d\tilde{e}$ into the left member of eqn (6) and solving it, the corresponding increment of the nondimensional curvature $d\tilde{k}$ is obtained. The optimum value of dk can be determined after examining all $d\tilde{k}$ values for each fiber element of the midsection and the straight segments.

The relative axial displacement, Δ, of the bar ends is given nondimensionally by the sum of the elastic–plastic extension of the bending portion and straight segments, and the axial component of the change in geometry:

$$\delta \equiv \Delta/(L\varepsilon_0) = \delta_B + \delta_R + \delta_G \tag{8}$$

$$\begin{cases} \delta_B = \xi e, \qquad \delta_R = (1-\xi)e_R \\ \delta_G = -\theta^2/(2\varepsilon_0) = -\alpha\xi k^2/(2n_c) \end{cases}$$
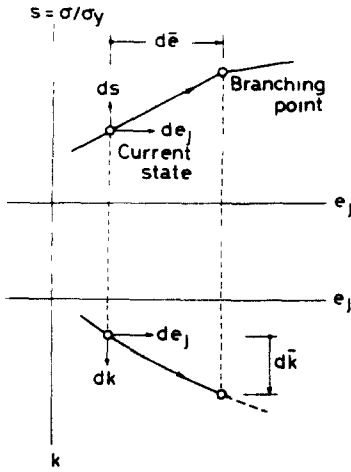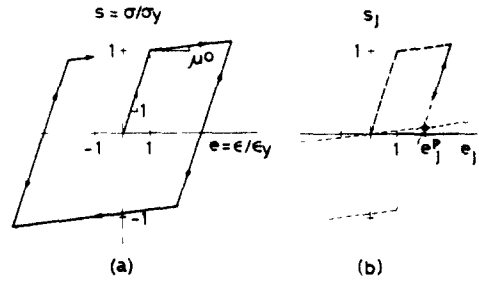
Fig. 3 Piecewise linear stress–strain relationship

Fig 4 Bi-linear stress–strain relationship

and all components are expressed incrementally as

$$d\delta_B = \xi\, de, \quad d\delta_R = (1-\xi)\, de_R$$
$$d\delta_G = -\alpha\xi/(2n_c)(2k+dk)\, dk. \tag{9}$$

If the bar is composed of an ideal I-section with bi-linear stress–strain relationship (Fig. 4), the closed-form solution of load-displacement relationship is obtained. In this case, e and k in eqn (8) are expressed by the simple functions of n, according to the stress states of both flanges (Table 1), where e_1^p and e_2^p denote the normalized plastic strains of each flange (Fig. 4b), μ^0 is the strain hardening ratio, and e_R is evaluated by n and the residual strain e_R^p.

$$e_r = \begin{cases} (n+1)/\mu^0-1: & n-\mu^0 e_R^p < -1 \\ n+(1-\mu^0)e_R^p: & |n-\mu^0 e_R^p| \leqq 1 \\ (n-1)/\mu^0+1: & n-\mu^0 e_R^p > 1. \end{cases} \tag{10}$$

Therefore, the nondimensional axial displacement δ is expressed in terms of n, in correspondence with values of e_1^p, e_2^p and e_R^p. The general hysteretic behavior of a bar of ideal I-section with bi-linear stress–strain relationship (Fig. 5), is discussed in the Appendix.

4. RESULTS AND DISCUSSIONS

The present analysis can be compared with the exact solution by Nonaka[3] for the elastic–perfectly plastic bar of ideal I-section (Fig. 6). $\xi = 1/3$ is the value that makes the central deflection of the model agree with that of a simply supported beam subjected to the concentrated lateral load at the center, and $\xi = 4/\pi^2$ corresponds to the value that makes the elastic buckling load of the model agree with the Euler load. In Fig. 6, $n - \delta$ is little dependent on the ξ value at the mechanism state in either the compression or tension range, but the elastic recovery lines and the total hysteretic behavior agree better with the exact solution for $\xi = 1/3$. It does, however, give about a 20% greater elastic buckling load than the Euler load for slender bars.

The validity of the present analysis depends greatly on the estimation of the ξ value, and ξ should be set to $\xi = 1/3$ because it gives a good estimation of the total hysteretic behavior. The mathematical appropriateness of this value will be discussed later.

The effect of the strain hardening is illustrated in Fig. 7. The hardening algebraically increases the loading capacity of stubby bars in the mechanism state, and has little effect on slender bars, as n_E is less than unity.

Table 1. Deformation characteristics for braces with varying state of stress

		FLANGE 2	
		ELASTIC	YIELDING IN TENSION
FLANGE 1	ELASTIC	**Case I** $k = \dfrac{n_c(1 - \mu^0)(e_2^P - e_1^P)}{2(n_c + n)}$ $e = n + (1 - \mu^0)(e_1^P + e_2^P)/2$	
	YIELDING IN TENSION	**Case II** $k = \dfrac{n_f(1 - \mu^0)(1 + \mu^0 e_2^P - n)}{2\mu^0(n_f + n)}$ $e = \dfrac{1}{1 + \mu^0}\left\{ 2n + (1 - \mu^0)(e_2^P - 1) - \dfrac{n_f(1 - \mu^0)^2(1 + \mu^0 e_2^P - n)}{2^0(n_f + n)} \right\}$	**Case IV** $k = 0$ $e = (n - 1)/\mu^0 + 1$
	YIELDING IN COMPRESSION	**Case III** $k = -\dfrac{n_f(1 - \mu^0)(1 - \mu^0 e_2^P + n)}{2\mu^0(n_f + n)}$ $e = \dfrac{1}{1 + \mu^0}\left\{ 2n + (1 - \mu^0)(e_2^P + 1) + \dfrac{n_f(1 - \mu^0)^2(1 - \mu^0 e_2^P + n)}{2\mu^0(n_f + n)} \right\}$	**Case V** $k = -\dfrac{n_c(1 - \mu^0)}{\mu^0 n_c + n}$ $e = n/\mu^0$

$$n_f = 2\mu^0 n_c/(1 + \mu^0)$$

The results of the step-by-step computation for a bar of rectangular cross section are compared with those of the one-dimensional finite element analysis[12] (Figs. 8 and 9). Two types of stress–strain relationships are assumed; one is the bi-linear type with hardening modulus, $10^{-4} \times E$ (Fig. 10a), which closely approximates the property of elastic–perfectly plastic material, and the other is the piecewise linear type (Fig. 10b), which approximates the hysteretic behavior of mild steel[15] (Fig. 10c). Because the Bauschinger's effect and the strain hardening are not taken into account (Fig. 8), when the axial force attains its limit value N_0, the bar becomes straight and the subsequent behavior takes the same pattern as the virgin state. Both curves agree well with each other, although some difference is seen for the stubby bar, where the present analysis slightly overestimates the deterioration of the hysteresis loop.

Figure 9 shows the results for the piecewise linear constitutive relationship. Because of the
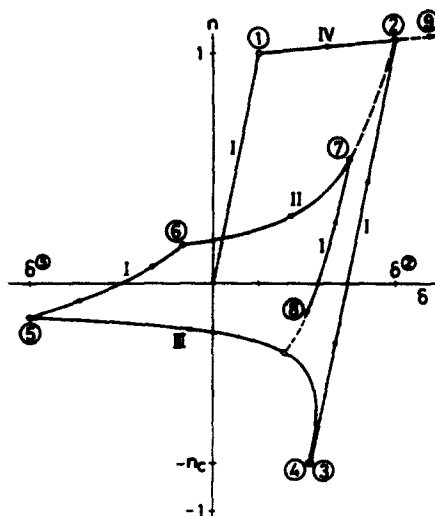

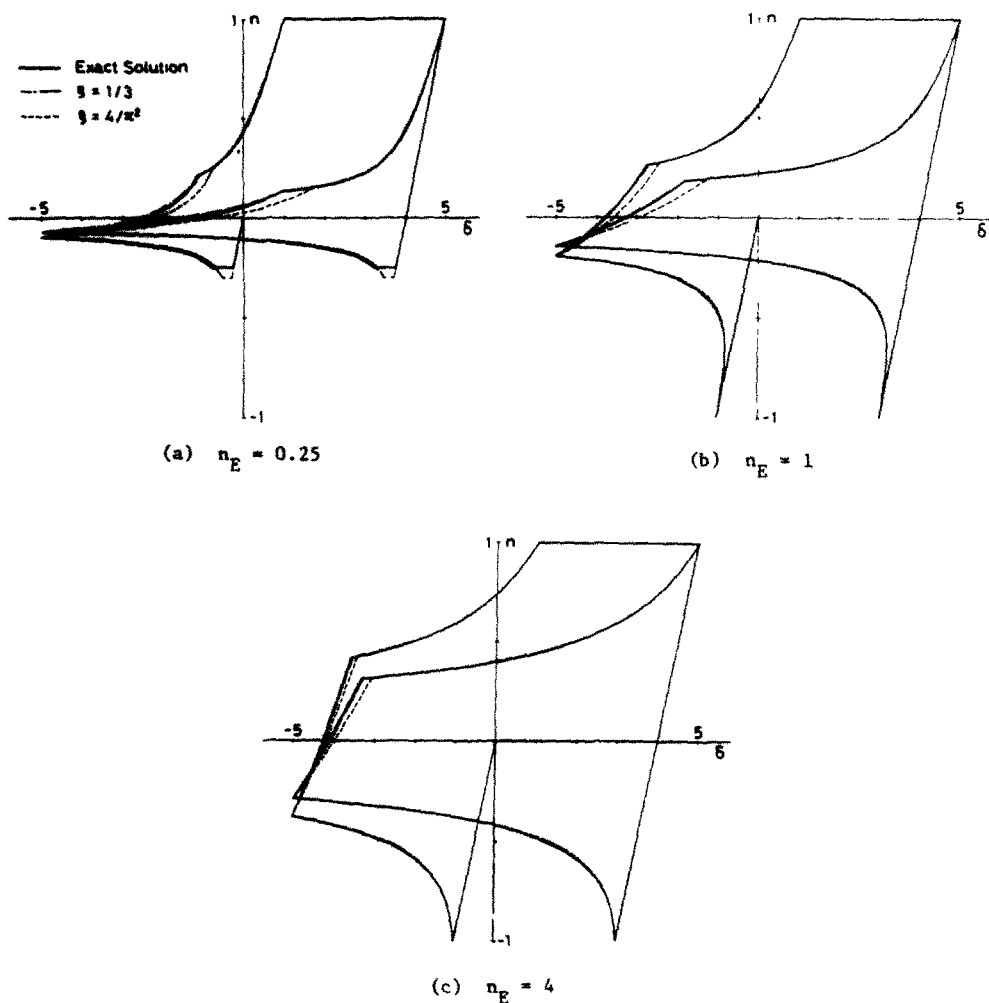Fig 5 Typical behavior of ideal I-section

(a) $n_E = 0.25$

(b) $n_E = 1$

(c) $n_E = 4$

Fig. 6. Comparision between present analysis and exact solution
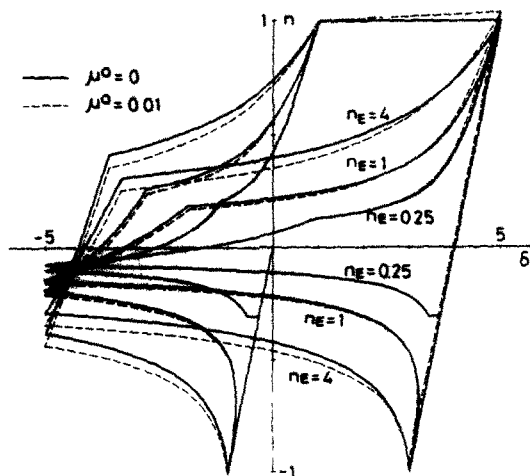

Fig 7 Effect of strain hardening
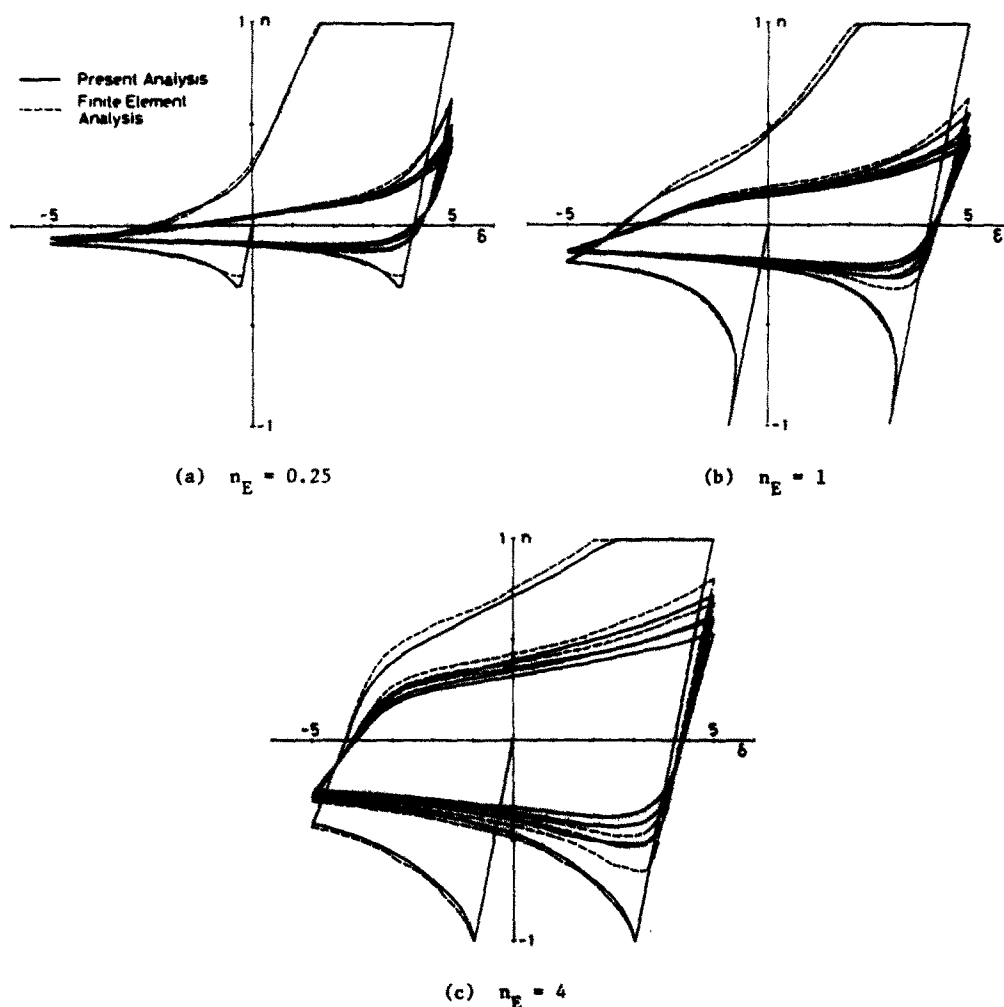
(a) $n_E = 0.25$

(b) $n_E = 1$

(c) $n_E = 4$

Fig. 8 Comparision between present analysis and finite element solution (Elastic–perfectly plastic stress–strain relationship.)

effect of strain hardening, the bar does not recover its straight configuration even if the axial force equals or becomes larger than N_0. The subsequent behavior differs greatly from that of the virgin state, as the Bauschinger's effect plays an important role. The hysteresis loop deteriorates with the increase of loading cycles more slowly than in the case of Fig. 8. The present analysis slightly underestimates the compression capacity as compared with the finite element solution.

The present analysis is in good agreement with the experimental results of Wakabayashi et al.[16] (Fig. 11).

5 FURTHER REMARKS

The validity of the analysis presented here depends on the selection of the ξ value. Setting $\xi = 1/3$, this analysis showed good agreement with the exact solution by Nonaka[4] for ideal I-section with elastic–perfectly plastic material, and with the detailed one-dimensional finite element analysis.

Those observations can be easily proved mathematically. According to Nonaka, the non-dimensional axial displacement is made up of the following components: the axial deformation at the plastic hinge, δ^p, the elastic–plastic elongation of the other portions, $(n + \delta^r)$, and the axial components of the change in geometry, δ^g [4]. The definition of δ^r agrees with that of $\bar{\delta}$ (see Appendix), and δ^g corresponds to δ_G. Let us introduce a new deformation parameter: $\delta_P = \delta_R + \delta_B - (n + \bar{\delta})$, which corresponds to δ^p in the exact solution.
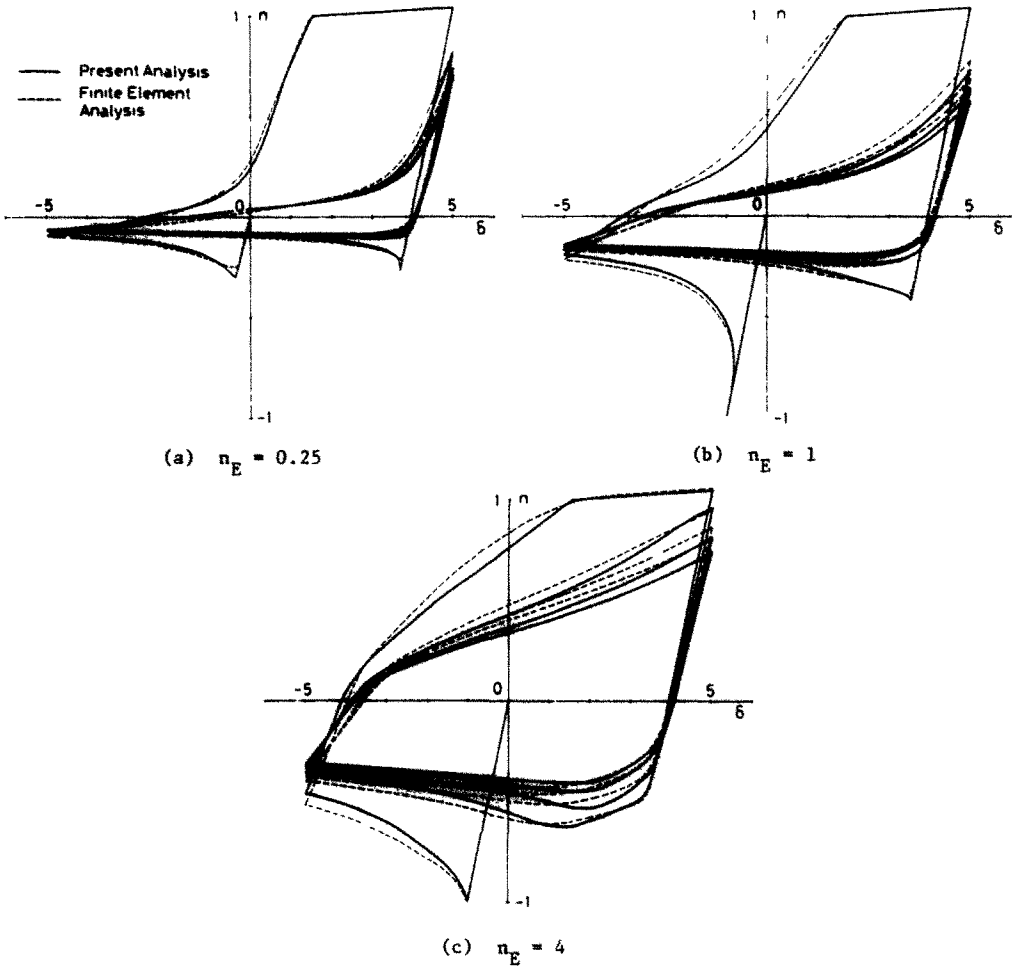
Fig. 9. Comparison between present analysis and finite element solution. (Piecewise linear stress–strain relationship.)

In the mechanism state in either the compression or tension range, δ_P and δ_G are evaluated as

$$\delta_P = -\frac{4n_E}{\pi^2}\frac{1-|n|}{|n|}\left(1+\frac{\xi\pi^2 n}{4n_E}\right) \tag{11}$$

$$\delta_G = -\frac{2n_E}{\pi^2}\left(\frac{1-|n|}{|n|}\right)^2. \tag{12}$$

For a slender bar, δ_G dominates the other components, and for a stubby bar, n/n_E takes a small value; $n-\delta$ at the mechanism does not depend so much on the value of ξ.

The exact solution yields the following expression for the mechanism state.

$$\delta^p = -\frac{1-|n|}{|n|} n \coth\left(\frac{\pi}{2}\sqrt{\left(\frac{n}{n_E}\right)}\right)\bigg/\left(\frac{\pi}{2}\sqrt{\left(\frac{n}{n_E}\right)}\right) \tag{13}$$

$$\delta^s = -\frac{(1-|n|)^2}{4n}\left\{\coth^2\left(\frac{\pi}{2}\sqrt{\left(\frac{n}{n_E}\right)}\right) + \coth\left(\frac{\pi}{2}\sqrt{\left(\frac{n}{n_E}\right)}\right)\bigg/\left(\frac{\pi}{2}\sqrt{\left(\frac{n}{n_E}\right)}\right) - 1\right\}. \tag{14}$$

Using the Taylor expansion for hyperbolic functions in eqns (13) and (14), we get

$$\delta^p = -\frac{4n_E}{\pi^2}\frac{1-|n|}{|n|}\left\{1+\frac{\pi^2 n}{12n_E} - \frac{1}{5}\left(\frac{\pi^2 n}{12n_E}\right)^2 + \cdots\right\} \tag{15}$$

$$\delta^s = -\frac{2n_E}{\pi^2}\left(\frac{1-|n|}{|n|}\right)^2\left\{1+\frac{1}{5}\left(\frac{\pi^2 n}{12n_E}\right)^2 - \cdots\right\} \tag{16}$$
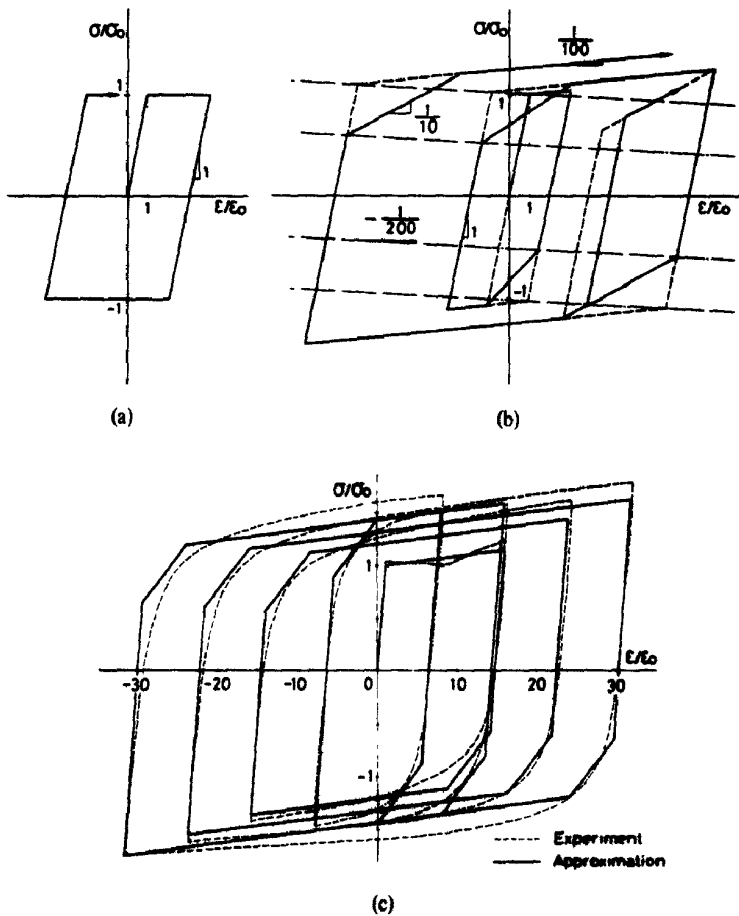
(a)   (b)

(c)

Fig. 10 Assumed stress–strain relationship

If we set $\xi = 1/3$, eqn (11) agrees with the first two terms of eqn (15), and eqn (12) agrees with the first term of eqn (16). In these equations the error introduced by neglecting the terms higher than the second order is less than 2%, if $n/n_E < 0.4$.

The relationship between $n^{\circledS}$ and $n^{\circledcirc}$ (Fig. 5) is obtained by setting $e - k = e_p^2 \pm 1$ in Case I in the Table:

$$\left(1 + \frac{1}{n^{\circledS}}\right)\left(1 + \frac{\xi \pi^2 n^{\circledS}}{4 n_E}\right) = \left(1 - \frac{1}{n^{\circledS}}\right)\left(1 + \frac{\xi \pi^2 n^{\circledcirc}}{4 n_E}\right). \tag{17}$$

The exact solution gives the relationship

$$\left(1 + \frac{1}{n^{\circledS}}\right)\frac{\pi}{2}\sqrt{\left(\frac{n^{\circledS}}{n_E}\right)} \coth\left(\frac{\pi}{2}\sqrt{\left(\frac{n^{\circledS}}{n_E}\right)}\right)$$

$$= \left(1 - \frac{1}{n^{\circledS}}\right)\frac{\pi}{2}\sqrt{\left(\frac{n^{\circledcirc}}{n_E}\right)} \coth\left(\frac{\pi}{2}\sqrt{\left(\frac{n^{\circledcirc}}{n_E}\right)}\right). \tag{18}$$

Expanding both members in Taylor series, we get

$$\left(1 + \frac{1}{n^{\circledS}}\right)\left\{1 + \frac{\pi^2 n^{\circledS}}{12 \cdot n_E} - \frac{1}{5}\left(\frac{\pi^2 n^{\circledS}}{12 \cdot n_E}\right)^2 + \frac{2}{35}\left(\frac{\pi^2 n^{\circledS}}{12 \cdot n_E}\right)^3 - \cdots\right\}$$

$$= \left(1 - \frac{1}{n^{\circledS}}\right)\left\{1 + \frac{\pi^2 n^{\circledcirc}}{12 n_E} - \frac{1}{5}\left(\frac{\pi^2 n^{\circledcirc}}{12 n_E}\right)^2 + \frac{2}{35}\left(\frac{\pi n^{\circledcirc}}{12 n_E}\right)^3 - \cdots\right\}. \tag{19}$$

If we set $\xi = 1/3$, both members of eqn (17) agree with the first two terms of both sides in eqn
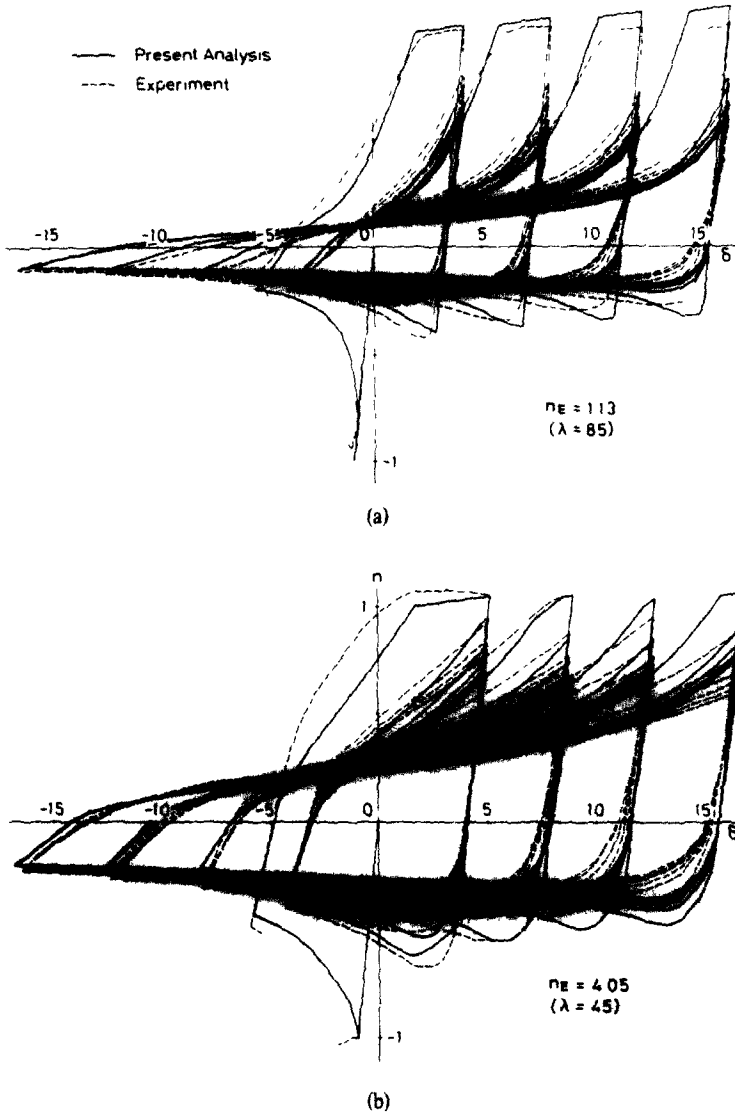
(a)

(b)

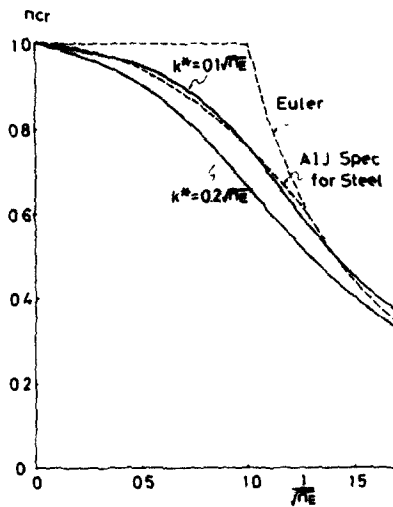Fig. 11 Comparision between present analysis and experimental result

Fig 12 Column curve

(19). Because the third terms of both members in eqn (19) almost cancel each other, the error produced by omitting the terms higher than the third order is less than 2%, if $n/n_E < 0.7$.

Although there remains concern that the elastic buckling load of the model is about 20% higher than the Euler load if $\xi = 1/3$, it may become trivial when the unavoidable imperfections are taken into account; the lack of straightness and the load eccentricity, for example. The initial curvature $k^* = 0.1\sqrt{(n_E)}$ corresponds to the central deflection $v \simeq (2L)/1200$ and $k^* = 0.2\sqrt{(n_E)}$ to $v \simeq (2L)/600$ The consideration of appropriate initial imperfections leads to a reasonable elastic buckling load in this analysis (Fig. 12).

The elastic-plastic spring idealization introduced in this paper can be applied to the response analysis[18], or to the problem with more complex boundary conditions[19, 20]. In the former, it dramatically reduces the computing time for determining the incremental load-displacement relationship, and in the latter case, it requires the appropriate estimation of the length of the bending portion An assemblage of several spring-bar units enable us to develop the one-dimensional finite-element solution[12], which proved the validity of the present analysis.

6 CONCLUSION

The hysteritic axial force-displacement relationship of a simply supported bar under repeated axial loading is analysed using the modified Shanley's model. The closed-form solution is obtained for the bar of ideal I-section with bi-linear stress-strain relationship. For a bar of arbitrary compact section with a general piecewise linear stress-strain relationship, an analytical expression is also derived for the incremental load-displacement relationship.

By solving for a bar of ideal I-section, the axial displacement is expressed as simple functions of the axial force. The functions do not include exponential or trigonometric functions as does the exact solution by Nonaka, and the axial force is obtained as the solution of a cubic equation for given axial displacement. The results for the bar with elastic-perfectly plastic material are in good agreement with those of the exact solution by Nonaka. The effect of the strain hardening can be easily taken into account.

The incremental method gives optimum increments of deformation parameters analytically without the trial-and-error process and consequently takes much less computing time. The computed results are in good agreement with the detailed finite element analysis and/or the experimental results.

REFERENCES

1 M Fujimoto, T Segawa and Y Matsumoto, An elastic-plastic analysis of a braced frame under repeated loading. *Abstracts. Ann Meeting Architectural Inst. Japan*, p. 1213 (1969)

2. S. Igarashi, K Inoue, M. Kibayashi and Y. Asano, Hysteretic characteristics of steel braced frames—Part 1. The behaviors of bracing members under cyclic axial forces *Trans Architectural Inst. Japan* (196), 47 (1972).

3 A B Higginbotham and R. D. Hanson, Axial hysteretic behavior of steel members. *J. Structural Div. Am. Soc. Civ. Engrs.* 102(ST7). 1365(1976)

4 T Nonaka, An elastic-plastic analysis of a bar under repeated axial loading. *Int. J. Solids Structures* 9, 569 (1973). (*Erratum* 10, 569(1973).)

5 T Nonaka, Approximations of yield condition for the hysteretic behavior of a bar under repeated axial loading *Int. Solids Structures* 13, 637 (1977)

6 T Nonaka, An analysis for large deformation of an elastic-plastic bar under repeated axial loading—I. Derivation of basic equations *Int J Mech. Sci* 19, 619 (1977)

7 T. Nonaka, An analysis for large deformation of an elastic-plastic bar under repeated axial loading—II. Correlation with small deformation theory. *Int. J. Mech Sci.* 19, 631(1977).

8 C. Matsui, I. Mitani and J. Tsumadori, Elastic-plastic analysis of a compressed steel brace. *Abstracts. Ann Meeting Architectural Inst Japan*, p 365 (1971)

9 Y Obama and J. Sakamoto, An analysis of the elastic-plastic behavior of steel braces *Abstracts Ann Meeting Architectural Inst. Japan*, p. 1369 (1972)

10 M Yamada and B Tsuji, Elasto-plastic behavior of bracings under the cyclic axial forces, Part 1 Analysis *Trans Architectural Inst Japan* (205), 31(1973)

11 M Fujimoto, A Wada, K Shirakawa and T Kosugi, Nonlinear analysis for K-type braced steel frames *Trans Architectural Inst Japan* (209), 41(1973)

12 M Wakabayashi and M Shibata, Studies on the post-buckling behavior of braces, Part 4. *Abstracts Ann Meeting Kinki Branch Architectural Inst Japan*, p. 201(1976)

13 F R Shanley, Inelastic column theory *J Aeronaut. Sci* 14(5), 261 (1947)

14 G Haaijer and B Thurlimann, On inelastic buckling in steel. *J Engng Mech Div Am Soc Civ. Engrs* 84(EM2),308 (1958).

15 Y Yokoo, T. Nakamura and T. Komiyama, Nonstationary hysteretic stress–strain relations of wide-flange steels and moment-curvature relations under presence of axial forces *Prelim Rep. Int Assoc. Bridge Struct. Engng Symp.* [*Lisboa*], p.145(1973)

16 M. Wakabayashi, T Nonaka, T Nakamura, S Morino and N. Yoshida, Experimental studies on the behavior of steel bars under repeated axial loading, *Ann. Disaster Prevention Res. Inst.* Kyoto University (16B), 113(1973)

17 Architectural Institute of Japan, *AIJ Standard for Structural Design of Steel Structures* (1970).

18. M. Shibata, Influence of restoring-force characteristics of braces on dynamic response of braced frame *Proc 7th World Conf. Earthquake Engng* [*Istanbul*] 4, 185 (1980)

19.M. Wakabayashi, M. Shibata and H. Masuda, An elastic-plastic analysis of a brace subjected to end constrains *Ann Disaster Prevention Res Inst*, Kyoto University (18b), 143(1975)

20 M Shibata and T Imamura, Elastic-plastic behavior of X-type braced frames, Part 2 *Abstracts Ann Meeting Architectural Inst. Japan*, p. 1413 (1978)

APPENDIX

Typical behavior of ideal I-section

Let us consider an example, in which the bar is at first subjected to elongation from the straight virgin state over the initial yield limit The behavior in this process is represented by the trace $\textcircled{0}$-$\textcircled{1}$-$\textcircled{2}$ in the n - δ relationship (Fig 5 in text) When the loading direction is reversed at state $\textcircled{2}$ and the bar is subjected to compression, the bar contracts without lateral deflection until the buckling load is attained The slender bar buckles elastically at $n = -n_c$, and enters into the mechanism state under the combined stress of bending and compression after flange 1 of the midsection yields in compression However, the stubby bar enters into the mechanism state immediately at $n = -1 + \mu^0 \bar{\delta}$, where $\bar{\delta} = \delta^{\textcircled{2}} - 1$ is the nondimensional residual displacement in the same sense as e^p defined in Fig. 3(b) in the text. In the case of $n_c = 0.5$, this process is denoted by the trace $\textcircled{1}$-$\textcircled{3}$-$\textcircled{4}$-$\textcircled{5}$ (Fig 5) In the mechanism state ($\textcircled{4}$-$\textcircled{5}$), the stress state of the midsection corresponds to Case III (Table 1) The plastic strains of flange 2 of the midsection and the straight segments are $e_2^p = e_R^p = \bar{\delta}$, and the normalized strain e_R of the straight segments is expressed according to the value of n_f

$$e_R = \begin{cases} n + (1 - \mu^0)\bar{\delta}, & n_f \leqq 1 \\[2mm] (n + 1)/\mu^0 - 1 & n_f > 1 \end{cases} \tag{A1}$$

Because we assumed that a too stubby bar is to be excluded from the analysis, let us restrict the discussion to the case of $n_f \leqq 1$

When the loading direction is reversed again, at stage $\textcircled{5}$ (Fig. 5), the bar behaves elastically, and e and k are expressed as Case I (Table 1) Because flange 2 of the midsection and the straight segments remain elastic before and after the load reversal, $e_2^p = e_R^p = \bar{\delta}$. Normalized plastic strain of flange 1 of the midsection e_1^p which should satisfy the condition $e_1 = e - k = e_1^p - 1$ at load reversal point $\textcircled{5}$— is obtained·

$$e_1^p = \frac{2(n_c + n^{\textcircled{5}})}{(1 + \mu^0)(n^{\textcircled{5}} + n_f)} \left[n^{\textcircled{5}} \left\{ 1 - \frac{1 - \mu^0}{n^{\textcircled{5}} + n_c} e_2^p \right\} + 1 \right] \tag{A2}$$

Increasing the tension force, n - δ attains the point $\textcircled{6}$, then flange 1 begins to yield in tension Solving for n in

$$\tilde{e}_1^p = \frac{2(n_c + n)}{(1 + \mu^0)(n + n_f)} \left[n \left\{ 1 - \frac{1 - \mu^0}{n + n_c} e_2^p \right\} - 1 \right] \tag{A3}$$

nondimensional axial force $n^{\textcircled{6}}$ at state $\textcircled{6}$ is obtained, where $e = e_1^p + 1$ is taken into account.

Beyond this state, the system moves into the mechanism state under combined stress of bending and tension, and n - δ is expressed by a curve toward point $\textcircled{2}$, which is the previous load-reversal point in the tension range. The stress state of the midsection is denoted as Case II in the Table. (If the contraction is increased more and more beyond state $\textcircled{5}$, flange 2 may yield in tension, and the stress state of the midsection may be expressed as Case V (Table 1). However, in this state the magnitude of the nondimensional axial displacement $|\delta|$ is more than twenty and is not realistic. Another assumption– flange 2 always remains elastic except for Case IV— is adopted in addition to those already stated in Section 2)

When the loading direction is reversed at state $\textcircled{7}$, the bar behaves elastically ($\textcircled{7}$-$\textcircled{8}$), and the plastic strain of flange 1 is obtained by substituting $n = n^{\textcircled{7}}$ into eqn (A3)

If the tension force is increased beyond state $\textcircled{7}$, flange 2 and the straight segments yield in tension at state $\textcircled{2}$, and the bar becomes straight. A further increase causes the n - δ relationship to trace the trajectry $\textcircled{7}$-$\textcircled{2}$-$\textcircled{9}$. e and k are expressed as Case IV (Table 1), and e_R is obtained by eqn (10c)

Under alternately repeated axial loading with constant displacement amplitude between $\delta^{\textcircled{2}}$ and $\delta^{\textcircled{5}}$, the lateral deflection vanishes at state $\textcircled{2}$ at each cycle, and the hysteresis loop stabilizes at the second cycle If loading direction is reversed from the stress state of Case V, after extremely increasing the contraction, the residual lateral deflection does not vanish at state $\textcircled{2}$, and the hysteresis loop under constant displacement amplitude deteriorates with the increase of the loading cycle